

Low-Cost Transfer Learning of Face Tasks

Thrupthi Ann John¹, Isha Dua¹, Vineeth N Balasubramanian², and C. V. Jawahar¹

¹IIT Hyderabad

²IIT Hyderabad

Abstract

Do we know what the different filters of a face network represent? Can we use this filter information to train other tasks without transfer learning? For instance, can age, head pose, emotion and other face related tasks be learned from face recognition network without transfer learning? Understanding the role of these filters allows us to transfer knowledge across tasks and take advantage of large data sets in related tasks. Given a pretrained network, we can infer which tasks the network generalizes for and the best way to transfer the information to a new task.

We demonstrate a computationally inexpensive algorithm to reuse the filters of a face network for a task it was not trained for. Our analysis proves these attributes can be extracted with an accuracy comparable to what is obtained with transfer learning, but 10 times faster. We show that the information about other tasks is present in relatively small number of filters. We use these insights to do task specific pruning of a pretrained network. Our method gives significant compression ratios with reduction in size of 95% and computational reduction of 60%

1. Introduction

Deep neural networks are very popular in machine learning, achieving state-of-the-art results in most modern machine learning tasks. A key reason for their success has been attributed to their capabilities to learn appropriate feature representations for a given task. The features of deep networks have also been shown to generalize across various tasks [28, 32], and learn information about tasks which they did not encounter during training. This is possible because tasks are often related, and when a deep neural network learns to predict a given task, the feature representations it learns can be adapted to other similar tasks to varying degrees. Several efforts in recent years [9, 14, 19, 49] have found such relationships between tasks that are diverse but

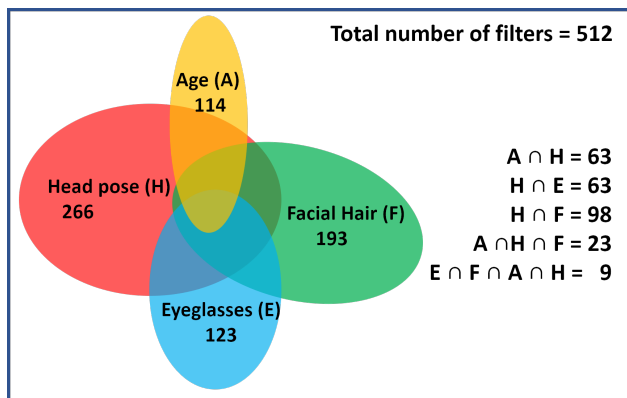


Figure 1. Figure depicts how information about different face tasks overlaps in the last convolutional layer of a face recognition network. The outer rectangle represents all the filters of the last layer, whereas the ovals depict the filters which contain information about different tasks. We observe that most of the tasks are encoded using very few filters, thus allowing us to compress the network by removing redundant filters.

related, such as object detection to image correspondence [19], scene detection to object detection [49] and expression recognition to facial action units [14].

One of the most important domains in computer vision is the face domain. Tasks in the face domain such as face recognition and emotion detection are very important in many applications such as biometric verification, surveillance and human-computer interaction. These tasks tend to be quite challenging, as face images can be similar to each other and face tasks often involve fine-grained classification. Besides, for a given face task, many variations need to be taken into account. For example, recognition has to be invariant to changes in expression, pose and accessories worn around the face. In recent years, we have seen that deep networks handle these challenging tasks very well. Deep Face Recognition [29] which trains a VGG-16[38] model on 2.6 million face images gives an accuracy of 97.27 on the LFW data set[13], whereas FaceNet[35] which uses

a pre-trained deep convolutional network to learn the embedding instead of an intermediate bottleneck layer gives an accuracy of 99.67%.

It is no new fact that tasks in the face domain are highly related to each other. As much as face tasks have to deal with many variations in images, from another perspective, different face tasks (such as face recognition, pose estimation, age estimation, emotion detection) operate on input data that are fairly similar to each other. These face tasks attempt to capture fine-grained differences between the images. Since the tasks are related and come from the same domain, one would expect that learning one task can help learn other tasks. We provide a simple generalizable framework to find relationships between face tasks, which can help models trained on a face task be transferred with very few computations to other face tasks.

One approach to achieve the aforementioned objective that has been studied in literature is multitask learning MTL [11, 31, 45, 48], where a single deep neural network is trained to solve multiple tasks given a single face image. An MTL architecture generally consists of a convolutional network which branches into multiple arms, each addressing a different face task. For example, Zhang *et al.* [48] estimate facial landmarks, head yaw, gender, smile and eye-glasses in a single deep model. These networks contain a large number of parameters and can be unwieldy to train. Furthermore, these methods require large data sets with labels for each of the considered tasks. In contrast, our studies on understanding what face networks learn and how they correlate with other face tasks, directly lend themselves to a method which can solve multiple tasks with far less labeled data and training overhead.

Our framework is pivoted on understanding the role and information contained in different filters in a convolutional layer with respect to other tasks that the base network was not originally trained for. Consider the last convolutional layer of the trained VGG-Face [29] model which has 512 convolutional filters. Different filters contain information about different face tasks. Figure 1 shows the distribution of these tasks in the 512 filters. We observe that while many filters are not relevant for other tasks, some filters are fairly general and can be easily adapted to solve other face tasks. Complementarily, we observe that when finetuning a pre-trained network for a different face task, the task-specific filters (that do not show relevance for use in the other task) can be removed, resulting in a highly streamlined network without much reduction in performance. We provide a pruning algorithm that removes these redundant filters so that the network can be used for a task it was not originally trained for. We achieve up to 98% reduction in size and 78% reduction in computational complexity with comparable performance.

Our key contributions are summarized as follows:

1. We introduce a simple method to analyze the internal representation of a pretrained face network and how information about other related tasks it was not trained for, is encoded in this network.
2. We present a computationally inexpensive method to transfer the information to other tasks without explicit transfer learning.
3. We show that information about other tasks is concentrated in very few filters. This knowledge can be leveraged to achieve cross-task pruning of pre-trained networks, which provides significant reduction of space and computational complexity.

2. Related Work

Deep neural networks achieve state-of-the-art results in many areas, but are notoriously hard to understand and interpret. There have been many attempts to shed light on the internal working of deep networks and the semantics of the features it generates. One class of methods [21, 23, 25, 26, 27, 40, 43] visualizes the convolutional filters of CNNs by mapping them to the image domain. Other works [8, 36, 37, 39, 50, 51] attempt to map parts of the image a network pays attention to, using saliency maps.

Other efforts attempt to interpret how individual neurons or groups of neurons work. Notably, the work by Raghu *et al.* [30] proposed a method to determine the true dimensionality of a layer and determined that it is much smaller than the number of neurons in that layer. S. Morcos *et al.* [34] studied the effect of single neurons on generalization performance by removing neurons from a neural network one by one. Alian and Bengio [2] developed intuition about the trained model by using linear classifiers that use the hidden units of a given intermediate layer as discriminating features. This allows the user to visualize the state of the model at multiple steps of training. D.Bau *et al.* [4] proposed a method for quantifying interpretability of latent representations of CNNs by evaluating the alignment between individual hidden units and a set of semantic concepts. These methods focus on interpreting the latent features of deep networks trained on a single task. In contrast, our work focuses on analyzing how the latent features contain information about external tasks which the network did not encounter during training, and how to reuse these features for these tasks.

We explore a simple alternative to transfer learning [5, 6, 7] in this work. In traditional transfer learning, a network is trained for a base task, its features are transferred to a second network to be trained on a target data set/task. There are several successful examples of transfer learning in computer vision including [3, 17, 28, 42]. Zamir *et al.* [47] used a computational approach to recommend the best transfer learning policy between a set of source and target

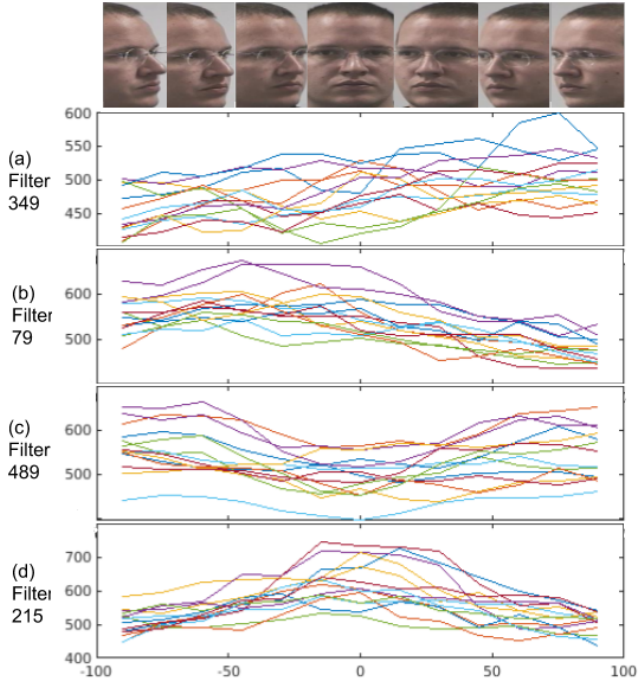


Figure 2. Figure shows the correlation between yaw angle on Head Pose Image Database and average responses of a few convolutional filters from the last layer of VGG-Face. The different lines in each graph represent 15 different identities: (a) high activation for left-facing faces; (b) high response for faces facing right; (c) high response for sideways faces; (d) high response for frontal faces

tasks. They also find structural relationships between vision tasks using this approach. Yosinski *et al.* [46] provided many recommendations for best practices in transfer learning. They quantified the degree to which a particular layer is general or specific, i.e., how well features at that layer transfer from one task to another. They also quantified the ‘distance’ between different tasks using a computational approach. In contrast, we provide a computationally cheaper alternative that emerges from understanding the filters of a convolutional network. We now present our motivation and methodology.

3. Learning Relationships between Face Tasks

It has been widely known in computer vision that CNNs learn generic features that can be used for various related tasks. For example, when a CNN learns to recognize faces, the convolutional filters may automatically learn to predict various other facial attributes such as head pose, age, gender etc. as a consequence of learning the face recognition task. These ‘shared’ filters can be reused for tasks other than what the network was trained for. This is our key idea.

We study the generalizability of such features using the following experiment. Consider the VGG-Face network

[29] trained for face recognition on 2.6 million images. We examine how the features of this network generalize to the task of determining head pose. The Head Pose Image Database [10] is a benchmark of 2790 monocular face images of 15 persons with pan angles from -90° to $+90^\circ$ at 15° intervals and various tilt angles. We use this data set because all the attributes are kept constant except for the head pose. We pass the images of the data set through the VGG-Face network and study the L_2 -norm of feature maps of each of the 512 filters in the last convolutional layer. We observe in Figure 2 that the response of certain filters are correlated to the yaw of the head. Some filters give high response for faces looking straight, whereas other filters give high response for left-facing faces. This experiment shows that few of the filters of a network trained for face recognition encode information about yaw without being explicitly trained for yaw angle estimation during training. This motivates the need for a methodology to identify and exploit the use of such filters to predict related tasks on which the original network was not trained.

Task	Type	Label Source
Identity	Categorical (10177 classes)	CelebA [18]
Gender	Categorical (2 classes)	CelebA[18]
Facial Hair	Multilabel (5 classes: 5 o'clock shadow, goatee, sideburns, moustache, no beard)	CelebA [18]
Accessories	Multilabel (5 classes: earrings, hat, necklace, necktie, eyeglasses)	CelebA [18]
Age	Categorical (10 classes)	Imdb-Wiki [33]
Emotions	Categorical (7 classes: angry, disgust, fear, happy, sad, surprise, neutral)	Fer13 [20]
Head pose	Categorical (9 classes)	3DMM[12]

Table 1. List of different tasks and corresponding labels. The labels for the first four tasks are provided with the CelebA data set. The other labels were obtained using known methods [12, 20, 33]

Methodology: Let a dictionary of face tasks be defined by $F = \{f_1, f_2, \dots, f_n\}$. Let f' be the primary task. Then the set of satellite tasks are denoted by $F - \{f'\}$. We train a network model \mathcal{M} on f' and use its features to regress for a satellite task $f^t \in F - \{f'\}$. For example, we can train a network on the primary task of face recognition and use its features to regress for satellite tasks such as age, head pose and emotion detection. To this end, we consider a con-

volutional layer of model \mathcal{M} with, say, k filters. Let the activation map of layer l on image I be denoted by $A^l(I)$, and has size $k \times u \times v$, where each activation map is of size $u \times v$. We hypothesize that, unlike contemporary transfer learning methodologies (that finetune the weights or input these activation maps through further layers of a different network), a simple linear regression model is sufficient to obtain the predicted label of the satellite task, f^t . Our procedure is outlined in Algorithm 1. First, we take the activation map of a convolutional layer and perform global average pooling on it. This is then used as a feature vector to regress the satellite tasks. Typically, a large data set is used to train the primary task, as with any other deep face network. However, owing to the simplicity of our satellite task model, limited data is sufficient to train the satellite model using linear regression.

Algorithm 1: Training Satellite Face Task Model from Primary Task Model

Input:

Face image data set for satellite task $f^t \in F - \{f'\}$:

$\{I_1, \dots, I_n\}$ with corresponding ground truth

$Y^t = \{y_1^t, \dots, y_n^t\}$

\mathcal{M} is a model obtained by training for the primary face task, f' .

$A^l(I_j)$ is the activation map (size $u \times v$) of layer l with k filters on image $I_j, j = 1, \dots, n$

Output: Regression model W^t for f^t

$$1 \quad W^t = \arg \min_W \sum_{j=1}^n \frac{1}{2} \|w^T A^l(I_j) - y_j^t\|^2$$

To validate the above mentioned method, a data set with ground truth for all considered face tasks is essential. We used the CelebA data set [18], which consists of 202,599 images all experiments in Section 3. The labels for identity, gender, accessories and facial hair are available as a part of the data set. For age, emotion and pose, we generated the ground truth using known methods. The ground truth for age was obtained using the method DEX: Deep EXpectation of apparent age from a single image [33]. This method uses a VGG16 architecture and was trained on the IMDB-WIKI data set which consists of 0.5 million images of celebrities crawled from IMDB and Wikipedia. The ages obtained using this method were binned into 10 bins, with each bin having 10 ages. Head pose was obtained by registering the face to a 3D face model using linear pose fitting [12]. The model used is a low-resolution shape-only version of the Surrey Morphable Face Model. The yaw and pitch values were binned into 9 bins ranging from top-left to bottom-right. The binned pose values are depicted in Figure 3. For emotion, a VGG-16 model was trained on FER 2013 data set [20] with 7 classes. (See Table 1 for the details of the considered data set).

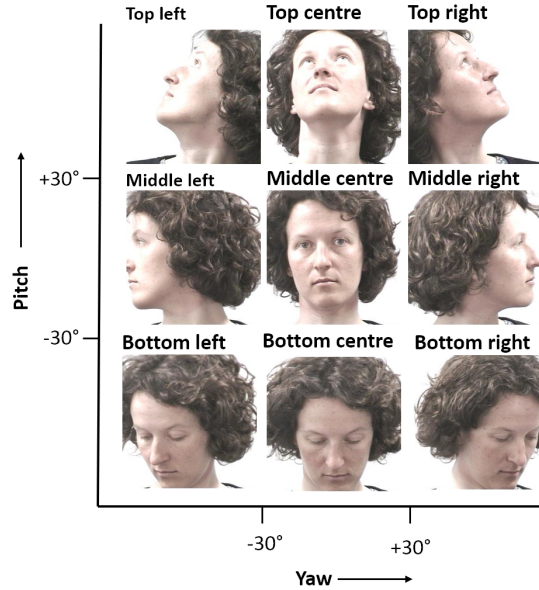


Figure 3. Classes for head pose task in Section 3. The yaw and pitch were divided into bins with 60° bin size.



Figure 4. Sample results obtained on CelebA data set using linear regression on the activation maps of a CNN trained for face recognition. Green text shows correct predictions, and red text shows incorrect predictions.

We consider the seven face tasks listed in Table 1. The entire CelebA data set was divided into 50% train, 25% validation and 25% test sets. We used a pre-trained VGG

	Age	Gender	Emotion	Facial Hair	Accessories	Pose
Face Recognition	42.5	97.1	46.21	94.34	92.65	85.22
Age	61.723	93.88	36.5	93.4	91.51	86.94
Gender	38.23	98.37	40.75	94.16	92.52	89.36
Emotion	29.21	87.8	69.014	91.88	91.16	87.48
Facial Hair	38.41	96.76	47.22	96.14	92.584	88.16
Accessories	38.26	96.46	39	93.56	94.76	87.77
Pose	36.90	95.05	40.79	93.38	93.43	96.62

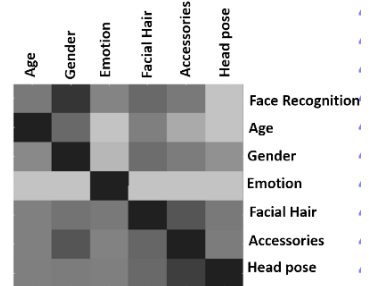


Figure 5. Table (left) shows results of transferring tasks using the proposed method. Each rows corresponds to the primary task and the columns correspond to the satellite task. We report the accuracy obtained when transferring a network pre-trained on the primary task to the considered satellite task. The diagonal cells show the accuracy obtained while training the primary task. The figure (right) shows a heatmap of transfer capability of one face task to another based on this methodology (darker is better; for example, face recognition models can regress gender very well, while age estimation models are one of the least capable of estimating emotions).

Face model [29] and finetuned it for a considered primary task. The ground truth for the satellite tasks were created by taking a subset consisting of 20,000 images from CelebA ($\approx 10\%$ of the data set). This was also divided into 50% train, 25% validation and 25% test sets. All our reported results are obtained by averaging over three random trials, obtained by different partitions of the satellite data. We converted the continuous regression outputs into categorical attributes for each of the tasks. For binary classes such as gender, our output was regressed to a value between 0 and 1, and a threshold (learned on the validation set) was used to decide the label on the test set. For multiclass classes such as age and pose, we regressed to a continuous label space based on the original labels. We then binned it using the same criteria we used for training the primary networks.

In order to determine how well a particular transfer took place, we compared the performance of our models learned on satellite tasks to the accuracy obtained by a network which was trained explicitly on the same task as primary. For example, say we want to compare the accuracy obtained by transferring a network trained for face recognition to the gender task. We do this by comparing the regression accuracy of face recognition \rightarrow gender with the network trained on the full data set for gender. This is measured as percentage reduction in performance when changing from the full data set to the subset.

Figure 5(left) shows the results of transferring tasks using regression. The activations were regressed to continuous labels, which were then binned to get the accuracy. For the emotion detection task, we used linear classification. The primary tasks are represented by each row, which was then transferred to each of the satellite tasks represented by the columns. The accuracy obtained by a network trained for the primary task is denoted in the cells where the primary and secondary task are the same. For each satellite task, percentage reduction in performance compared to the network trained on the corresponding primary task is also

captured in Figure 5 (right), with lower values (darker cells) being better. We show some qualitative results obtained using our regression algorithm in Figure 4.

We notice that networks trained on primary tasks give better results while regressing with tasks with which the primary tasks may have some correlation. For example, a model trained on gender recognition as the primary task gives good results for facial hair estimation and vice versa (supports common knowledge). Similarly, the accessories and gender estimation tasks are strongly correlated because certain accessories such as neck tie, earrings, and necklace are correlated strongly with gender. On the other hand, emotion gives low accuracy for all other tasks, since emotion is usually learned independently from other facial attributes. Face recognition gives very good results for gender, facial hair and accessories since these vary from individual to individual. Face recognition does not give the best results for pose, because face recognition has to be invariant to pose. Curiously, age is regressed well by the face recognition network. This may be due to biases in the data set, where images belonging to each individual do not have a large range of ages.

Relation to Transfer Learning: We conducted experiments to examine how well our regression method compares to using transfer learning on various tasks. For this setting, we used networks pretrained on the face recognition tasks and reinitialized all the fully connected layers. We then froze the convolutional layers and trained the linear layers for the satellite tasks. The results can be seen in figure 6. We can see that the regression results are close to the transfer results. Thus, we can use our simple regression method to find task relationships instead of doing expensive transfer learning for each task. Our regression method takes 10 seconds to run for a single task, as opposed to transfer learning, which takes 780 seconds. We thus achieve a speed-up of **78X** using our method.

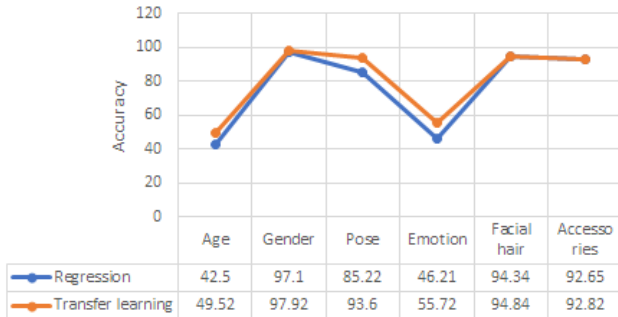


Figure 6. Graph shows comparison between regression and transfer learning for a network pretrained on face recognition and transferred to six other tasks. We can see that results for regression and transfer learning are very close, thereby allowing us to effectively replace transfer learning with our method.

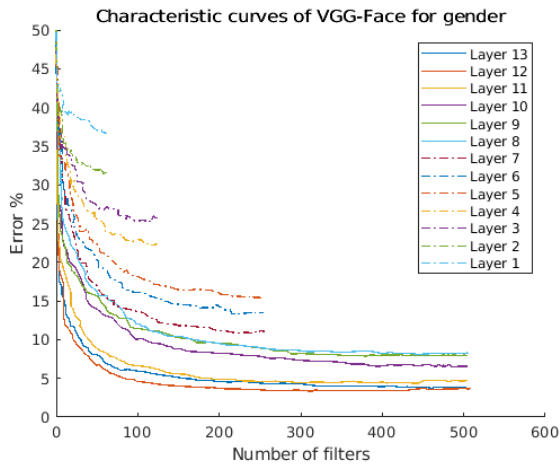


Figure 7. Characteristic curves for VGG-Face pretrained network regressed on gender. We can observe that regression gives very low error using as few as ~ 100 filters. Adding more filters to the regression model does not have a large impact on the error, indicating that the additional filters do not capture much information about gender

4. Pruning across Face Tasks

Motivation: We have seen how the filters of convolutional layer of a pretrained network trained for one task can be repurposed for another. All filters of a layer may not have equal importance in terms of usefulness for predicting the satellite task. In order to discover which filters from the layer are useful for the task and which filters are redundant, we need to rank every group of filters according to the accuracy obtained on regressing to the satellite task. Instead of exhaustively checking all groups of filters in a layer, we use feature selection to achieve this. In particular, we use LASSO [41], a L_1 -regularized regression method which selects only a subset of the variables in the final model rather than using all of the variables using the objective:

$$\min_{\beta_0, \beta} \left(\frac{1}{2N} \sum_{i=1}^N (y_i - \beta_0 - x_i^T \beta_i^T)^2 + \lambda \sum_{j=1}^p |\beta_j| \right) \quad (1)$$

where N is the number of observations, y_i is the dependent variable at observation i , x_i is the independent variable (a vector of globally averaged filter responses at observation i) and λ is a non-negative regularization parameter which determines the sparseness of the regression weights β .

As λ increases, the number of filters chosen decreases, which are the non-zero coefficients of β . We train lasso using 100 different values of λ to get a characteristic curve. The largest value of λ is one that just makes all coefficients zero. The rest of the λ values are chosen using a geometric sequence such that the ratio of largest to smallest λ is $1e4$. For each layer, we get 100 regression models, each using different number of filters. The root mean squared error of the regression models is plotted with respect to the number of filters to obtain the characteristic curve of the layer.

The characteristic curves of a network with respect to a satellite task T tell us how the information about T is distributed in the network. Let us observe the characteristic curves for VGG-Face pretrained network regressing on gender in Figure 7. We can see that the error drops significantly using just a few filters and remains constant after that. This indicates that most of the information about gender is present in a few filters and the other filters are not needed for this task. We can use this fact to do cross-task pruning of the network by removing redundant filters.

More examples of characteristic curves are given in figure 8. Figure 8A shows the characteristic curves obtained for VGG-Face pretrained network for the yaw task. These curves are quite sharp in the beginning, indicating that the yaw information is encoded by a few neurons. When we compare these to the characteristic curves of valence for VGG-Face network in Figure 8C, we notice that these curves are very smooth and there is no elbow, showing that the information about valence is distributed throughout the layers. This is reflected by the compression ratios obtained while pruning for these tasks. (Refer to Table 2).

Pruning from Filters: The main goal of pruning is to reduce the size and computational complexity without much reduction in performance. Our pruning algorithm has two steps: 1. Remove top layers of the network which give less performance 2. For each layer, retain only filters that have information about task T . We use the characteristic curves as a guide for choosing which filters to keep and which to prune. We choose a knee-point for the characteristic curve of a layer in order to balance the number of filters and performance. The knee-point is defined as the minimum number of filters such that increase in RMSE is not more than a threshold. We have to minimize the number of features

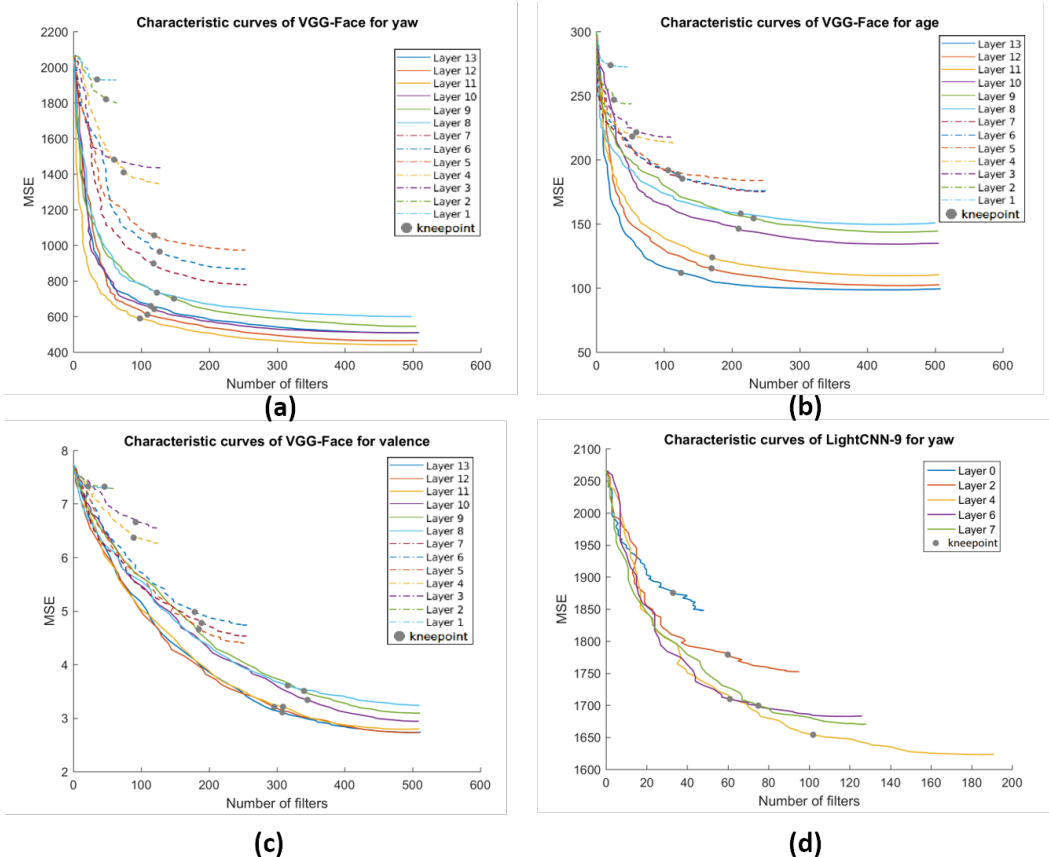


Figure 8. Characteristic curves obtained while regressing the primary network for various satellite tasks. The kneepoints indicate the regression model corresponding to threshold = 0.01. a.) VGG-Face regressed for head pose using AFLW data set [22] b.) VGG-Face regressed for age using AgeDB [24] c.) VGG-Face regressed for valence (emotion) using AFEW-VA data set [15, 1] d.) LightCNN face network [44] regressed for head pose using AFLW data set.(Zoom in to see the details)

such that

$$\text{RMSE}(k) - \min(m) < \gamma(\max(m) - \min(m)) \quad (2)$$

where m is the RMSE at a point on the curve, k is the chosen knee-point and $\text{RMSE}(k)$ is the RMSE at the kneepoint. γ is a threshold expressed as a percentage of the range of RMSEs of a layer. We keep all the filters which are chosen by the regression model at k , and discard the rest using the procedure described in [16].

Let a convolutional layer l have o_l filters and i_l input channels. The weight matrix of the layer will have the dimensions $o_l \times i_l \times k_l \times k_l$ (where $k_l \times k_l$ is the kernel size). Our procedure to prune filters from layer l is shown in Algorithm 2.

In order to extend our pruning algorithm to architectures that are very different to VGG architecture, we have to modify the filter pruning procedure. Here, we examine the procedure to prune LightCNN-9 architecture. LightCNN introduces an operation called Max-Feature-Map (MFM) operation. An MFM 2/1 layer which has i_l input channels and o_l

output channels has two components: a convolutional layer which has i_l input channels and $2o_l$ output channels, and the MFM operator which combines the output channels using max across channels so that the output of the entire layer has only o_l channels. Let the output X of the convolutional layer have dimensions $2o_l \times h \times w$. The MFM operator is defined as:

$$\hat{x}_{i,j}^p = \max(x_{i,j}^p, x_{i,j}^{p+o_l}) \quad (3)$$

where $\hat{x}_{i,j}^p$ is the $(i,j)^{\text{th}}$ element of channel k of the output. If we want to keep $D = \{f_1, f_2, \dots, f_d\}$ channels out of o_l channels, we need to keep both D and $D + o_l$ output channels from the convolutional layer and corresponding input channels from the next layer.

LightCNN also has group layers which consist of two MFM layers. Consider a group layer with i_l input channels, o_l output channels and $k \times k$ filter size. The first MFM layer has 1×1 convolutional layer with i_l input layers and i_l output layers. The second MFM layer has i_l input channels, o_l output channels and $k \times k$ convolutional size. In order to keep D filters in a group, we keep D filters from the second

Attribute	Arch	RMSE	FLOP	% FLOP reduction	Parameters	% Size reduction
Yaw	VGG-Face	38.97	2.54×10^{11}	65.53	2.03×10^7	96.50
Age	VGG-Face	14.28	3.28×10^{11}	55.57	2.61×10^7	95.49
Valence	VGG-Face	1.93	5.53×10^{11}	25.03	4.41×10^7	92.39
Yaw	LightCNN	40.42	7.09×10^9	78.9	1.42×10^6	98.62

Table 2. Table showing results of pruning, along with space and time compression ratios achieved by it.

Algorithm 2: Prune filters from a layer in a network

Input: layer l , next convolutional layer $l + 1$, kn :
knee-point of the characteristic curve of layer l (Equation 2)

Output: Network with layers l and $l + 1$ pruned

- 1 $W_l \leftarrow$ weights corresponding to the regression model at the knee-point.
 - 2 $n_l \leftarrow$ number of non-zero elements of W_l
 - 3 Let convolutional layer l have o_l filters and i_l filters of size $k_l \times k_l$. Create a new convolution layer with n_l filters. Its weight matrix is of size $n_l \times i_l \times k_l \times k_l$
 - 4 **for** each non-zero element i in W_l **do**
 - 5 **for** $j = 1:n_l, p = 1:i_l, q = 1:k_l, r = 1:k_l$ **do**
 - 6 newweights[j, p, q, r] \leftarrow oldweights[i, p, q, r]
 - 7 **end**
 - 8 **end**
 - 9 Replace layer l with new convolutional layer
 - 10 **if** conv layer $l+1$ exists **then**
 - 11 Create a new convolution layer with n_l input channels.
 - 12 **for** each non-zero element i in W_{l+1} **do**
 - 13 **for** $p = 1:o_{l+1}, j = 1:n_l, q = 1:k_l, r = 1:k_l$ **do**
 - 14 newweights[p, j, q, r] \leftarrow oldweights[p, i, q, r]
 - 15 **end**
 - 16 **end**
 - 17 Replace layer $l + 1$ with the new layer
 - 18 **end**
-

MFM layer (as detailed above). We also keep D filters from the first MFM layer of the next group.

Results: Our pruning experiments are conducted on various data sets other than CelebA in order to determine if our insights can be adapted to other data sets. Our base network is the VGG-Face network [29], which we prune so that it can be reused for head pose, age and emotion (valence). We use Annotated Facial Landmarks in the Wild (AFLW) [22] data set for pose task. AFLW contains a large number of ‘in the wild’ faces for which yaw, pitch and roll attributes are provided. We only use yaw values for our experiments.

For age prediction task, we use AgeDB data set [24], which has more than 15000 images with ages ranging from

Type	Gender		
	Filter size/stride,pad	Output size	#param
Conv2D	3 × 3 / 1,1	224 × 224 × 58	6.4K
ReLU	-	224 × 224 × 58	-
Conv2D	3 × 3 / 1,1	224 × 224 × 54	112.9K
ReLU	-	224 × 224 × 54	-
MaxPool	2 × 2 / 2,0	112 × 112 × 54	-
Conv2D	3 × 3 / 1,1	112 × 112 × 109	212.3K
ReLU	-	112 × 112 × 109	-
Conv2D	3 × 3 / 1,1	112 × 112 × 114	447.8K
ReLU	-	112 × 112 × 114	-
MaxPool	2 × 2 / 2,0	56 × 56 × 114	-
Conv2D	3 × 3 / 1,1	56 × 56 × 216	887.3K
ReLU	-	56 × 56 × 216	-
Conv2D	3 × 3 / 1,1	56 × 56 × 223	1734.9K
ReLU	-	56 × 56 × 223	-
Conv2D	3 × 3 / 1,1	56 × 56 × 232	1863.4K
ReLU	-	56 × 56 × 232	-
MaxPool	2 × 2 / 2,0	28 × 28 × 232	-
Conv2D	3 × 3 / 1,1	28 × 28 × 373	3116.8K
ReLU	-	28 × 28 × 373	-
Conv2D	3 × 3 / 1,1	28 × 28 × 373	5010.1K
ReLU	-	28 × 28 × 373	-
Conv2D	3 × 3 / 1,1	28 × 28 × 379	5090.7K
ReLU	-	28 × 28 × 379	-
MaxPool	2 × 2 / 2,0	14 × 14 × 373	-
Conv2D	3 × 3 / 1,1	14 × 14 × 302	4121.7K
ReLU	-	14 × 14 × 302	-
Conv2D	3 × 3 / 1,1	14 × 14 × 309	3360.6K
Avg. pool	-	309	-
Linear	-	2	2.4K

Table 3. The Architecture of VGG-Face network after pruning for gender

1 to 101. The valence task is analyzed using AFEW-VA data set [1, 15]. This data set consists of clips extracted from feature films that have per frame annotation of valence and arousal. The data sets are randomly split into 75% for training and 25% for testing. We perform the pruning experiments on VGG-Face [29] for yaw, age and valence tasks. The results are given in Table 2. We can see that the computation and size of networks have been significantly reduced, while the error is less than the network that was trained from scratch. There are several reasons for this. First, the fully connected layers are removed, which reduces the number of parameters by a great amount. Next, as we can see from Figure 7, the information pertaining to satellite tasks are concentrated in very few neurons in VGG-Face network. Hence we are able to remove many convolutional filters from each layer without impacting the performance much. For valence, the information is spread throughout

Type	Age		
	Filter size/stride,pad	Output size	#param
Conv2D	3 × 3 / 1,1	224 × 224 × 60	6.7K
ReLU	-	224 × 224 × 60	-
Conv2D	3 × 3 / 1,1	224 × 224 × 58	125.5K
ReLU	-	224 × 224 × 58	-
MaxPool	2 × 2 / 2,0	112 × 112 × 58	-
Conv2D	3 × 3 / 1,1	112 × 112 × 79	165.2K
ReLU	-	112 × 112 × 79	-
Conv2D	3 × 3 / 1,1	112 × 112 × 105	299K
ReLU	-	112 × 112 × 105	-
MaxPool	2 × 2 / 2,0	56 × 56 × 105	-
Conv2D	3 × 3 / 1,1	56 × 56 × 201	760.5K
ReLU	-	56 × 56 × 201	-
Conv2D	3 × 3 / 1,1	56 × 56 × 220	1592.8K
ReLU	-	56 × 56 × 220	-
Conv2D	3 × 3 / 1,1	56 × 56 × 240	1901.7K
ReLU	-	56 × 56 × 240	-
MaxPool	2 × 2 / 2,0	28 × 28 × 240	-
Conv2D	3 × 3 / 1,1	28 × 28 × 396	3423.0K
ReLU	-	28 × 28 × 396	-
Conv2D	3 × 3 / 1,1	28 × 28 × 449	6402.7K
ReLU	-	28 × 28 × 449	-
Conv2D	3 × 3 / 1,1	28 × 28 × 387	6257.0K
ReLU	-	28 × 28 × 387	-
MaxPool	2 × 2 / 2,0	14 × 14 × 387	-
Conv2D	3 × 3 / 1,1	14 × 14 × 332	4626.7K
ReLU	-	14 × 14 × 332	-
Conv2D	3 × 3 / 1,1	14 × 14 × 350	4184.6K
ReLU	-	14 × 14 × 350	-
Conv2D	3 × 3 / 1,1	14 × 14 × 275	3466.1K
Avg. pool	-	275	-
Linear	-	10	11.04K

Table 4. The Architecture of VGG-Face network after pruning for age

the network, hence the compression ratio is less than that of yaw and age. The architectures of the pruned networks are given in Tables 3, 4, 5 and 6.

Table 2 also shows the results of our pruning method on LightCNN architecture, in order to show that our algorithm is applicable for a variety of architectures. We pruned LightCNN network pretrained on face recognition for yaw tasks. As can be seen from Table 2, the algorithm works equally well for LightCNN architecture.

We also show results of finetuning the pruned networks on the data sets of the satellite tasks. This allows us to get an accuracy similar to the uncompressed network. The networks were pruned with threshold values of 0.1, 0.01 and 0.001 (See Equation 2). The results are shown in Figure 9. We observe that as threshold increases, the network size and computational complexity reduces significantly while retaining the accuracy. Thus, threshold is a reliable way to tune the pruning algorithm and get the desired compromise between compression ratio and accuracy. We also note that the best threshold for all tasks is 0.01, as it gives a good trade-off between accuracy and compression ratio. The inference time of compressed networks is 10 times faster than the original networks, while giving similar accuracy, as seen

Type	Head pose		
	Filter size/stride,pad	Output size	#param
Conv2D	3 × 3 / 1,1	224 × 224 × 23	2.5K
ReLU	-	224 × 224 × 23	-
Conv2D	3 × 3 / 1,1	224 × 224 × 12	9.984K
ReLU	-	224 × 224 × 12	-
MaxPool	2 × 2 / 2,0	112 × 112 × 12	-
Conv2D	3 × 3 / 1,1	112 × 112 × 121	52.756K
ReLU	-	112 × 112 × 121	-
Conv2D	3 × 3 / 1,1	112 × 112 × 110	479.6K
ReLU	-	112 × 112 × 110	-
MaxPool	2 × 2 / 2,0	56 × 56 × 110	-
Conv2D	3 × 3 / 1,1	56 × 56 × 234	927.5K
ReLU	-	56 × 56 × 234	-
Conv2D	3 × 3 / 1,1	56 × 56 × 230	1938.4K
ReLU	-	56 × 56 × 230	-
Conv2D	3 × 3 / 1,1	56 × 56 × 227	1880.4K
ReLU	-	56 × 56 × 227	-
MaxPool	2 × 2 / 2,0	28 × 28 × 227	-
Conv2D	3 × 3 / 1,1	28 × 28 × 370	3025.1K
ReLU	-	28 × 28 × 370	-
Conv2D	3 × 3 / 1,1	28 × 28 × 348	4636.7K
ReLU	-	28 × 28 × 348	-
Conv2D	3 × 3 / 1,1	28 × 28 × 390	4887.4K
ReLU	-	28 × 28 × 390	-
MaxPool	2 × 2 / 2,0	14 × 14 × 390	-
Conv2D	3 × 3 / 1,1	14 × 14 × 362	5083.9K
ReLU	-	14 × 14 × 362	-
Conv2D	3 × 3 / 1,1	14 × 14 × 395	5149.2K
ReLU	-	14 × 14 × 395	-
Conv2D	3 × 3 / 1,1	14 × 14 × 409	5817.6K
Avg. pool	-	409	-
Linear	-	9	14.76K

Table 5. The Architecture of VGG-Face network after pruning for head pose

in Figure 10.

5. Discussion

Key Observations: Some of our major observations can be summarized as follows:

- We can adapt the features learned by a deep network for a task it was not trained for, without having access to the original data set. The complex features learned on a large data set can be leveraged for tasks for which large data sets are not available. This works well in practice.
- Most of the face tasks are highly related to each other. Thus we can easily transfer knowledge among them. Models learned on certain tasks such as face recognition are very versatile and give good accuracy when transferred to other tasks. Emotion detection models are not very useful for transferring to other face tasks (and seem to be largely on their own in our list of face tasks).
- The information pertaining to other tasks is encoded by very few filters in each layer of a network. thus in

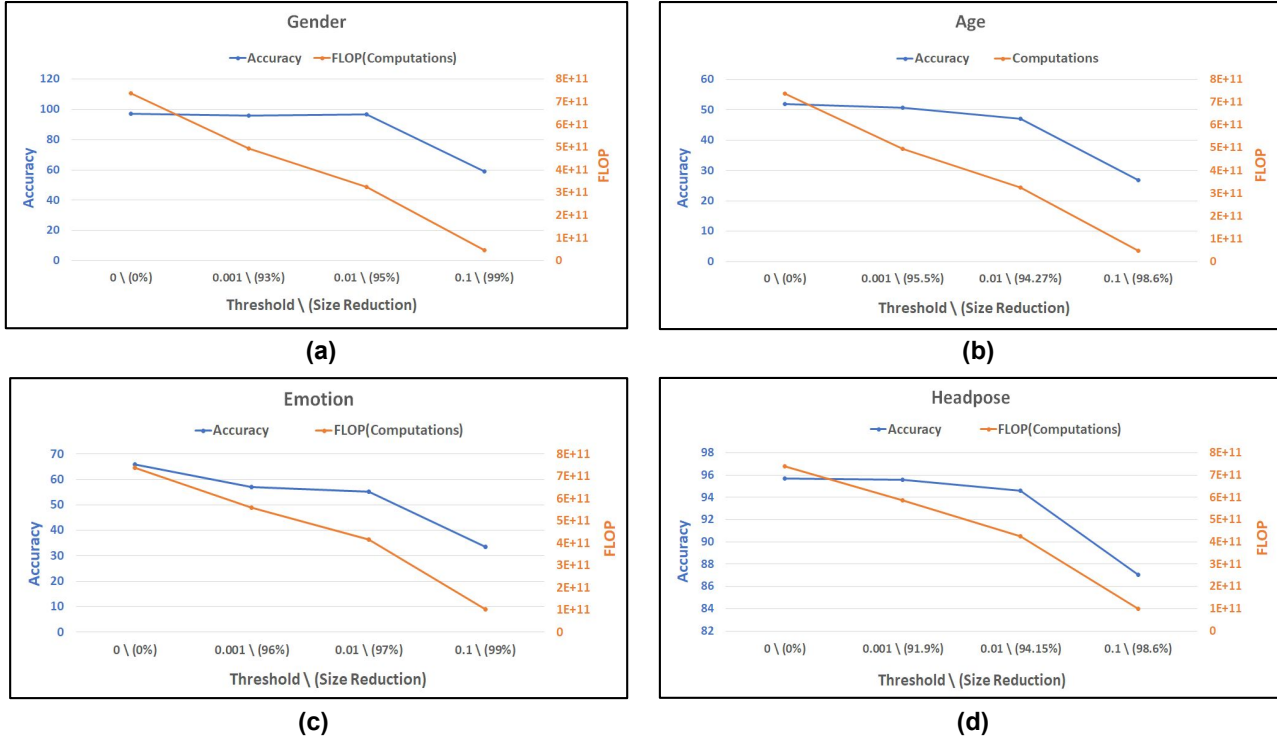


Figure 9. The four figures show the accuracy and computational complexity for VGG-Face network pruned with different thresholds. For each task, the threshold was varied from 0.1 to 0.001. A threshold of 0 indicates the finetuned network which is not pruned. We have shown the accuracy on the left axis and computational cost (number of flops) on the right axis. The percentage reduction in size is given along with the respective threshold values on the X-axis. a) Gender b) Age c) Emotion d) Head pose

most cases, we achieve very high level of compression by removing redundant filters.

- This pattern of having few useful filters is present in other architectures such as LightCNN [44] and networks trained using other loss functions. Our approach corroborates these earlier efforts, and provides a simple methodology to adapt this insight for cross-task pruning.

Performance of Different Convolutional Layers: A network with VGG-16 architecture has 13 convolutional layers. We now try to ask: which layer gives the best results for transferring information to other tasks in our approach? Our regression experiments were conducted on all the convolutional layers of the network and best results were recorded. The accuracy for the last 6 layers for different tasks is given in Figure 11. The layer which gives the best result varies for different satellite tasks, as expected. For instance, head pose, gender and age are best learned from layer 13 while the task emotion is best learned from layer 10. The layer in which task is learned with best accuracy signifies its relation with the primary task.

Extension to Different Data Sets, Tasks and Architectures: Our framework can easily be extended to data sets and tasks other than what is explored in this paper. It can also be applied to any pre-trained network, even if we do not have the original data set it was trained for. In Section 4, we use a pretrained VGG-Face network [29] as our base network. All the satellite tasks were on varied data sets, showing that our framework can be extended to other CNN architectures, by finding redundant filters and removing them.

Applications and Future Directions: The knowledge of the various tasks encoded by different filters opens up a lot of opportunities. This can be very useful for finetuning and transfer learning. Before training the network, determine which filters are needed and remove the rest of the filters. This reduces the resources and time needed for training. We can also use this knowledge to customize networks in creative ways. For example, if we want to train a network for emotion and render it agnostic to face identity, we can find which filters represent identity and remove those filters to get an identity-agnostic network.

In total, we trained 180 networks which took approxi-

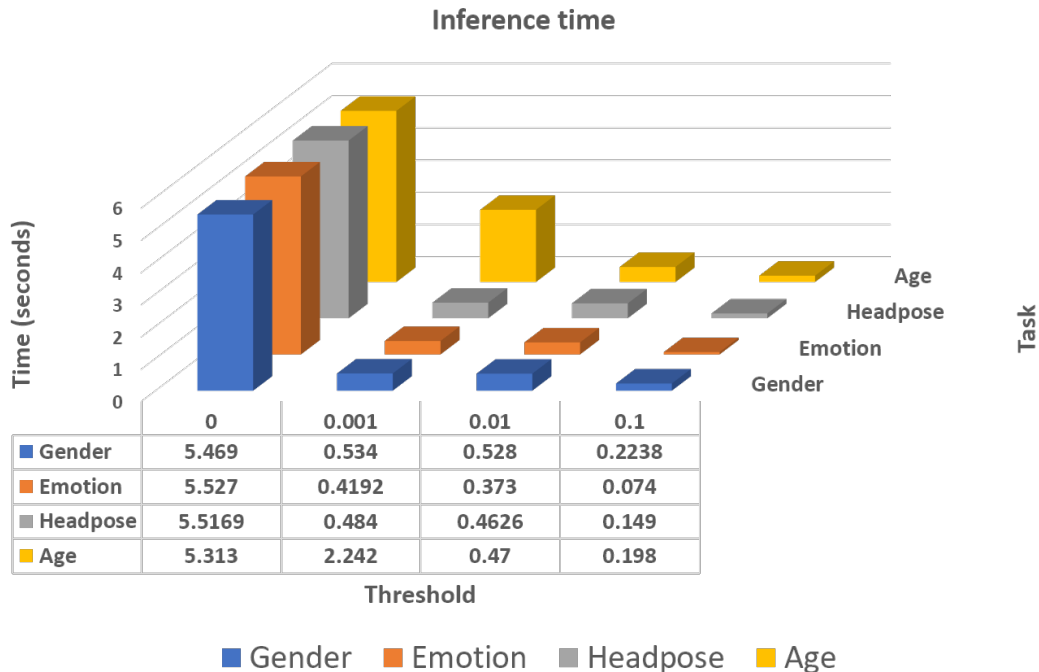


Figure 10. Time for inference of one image on the CPU for the full network versus pruned networks.

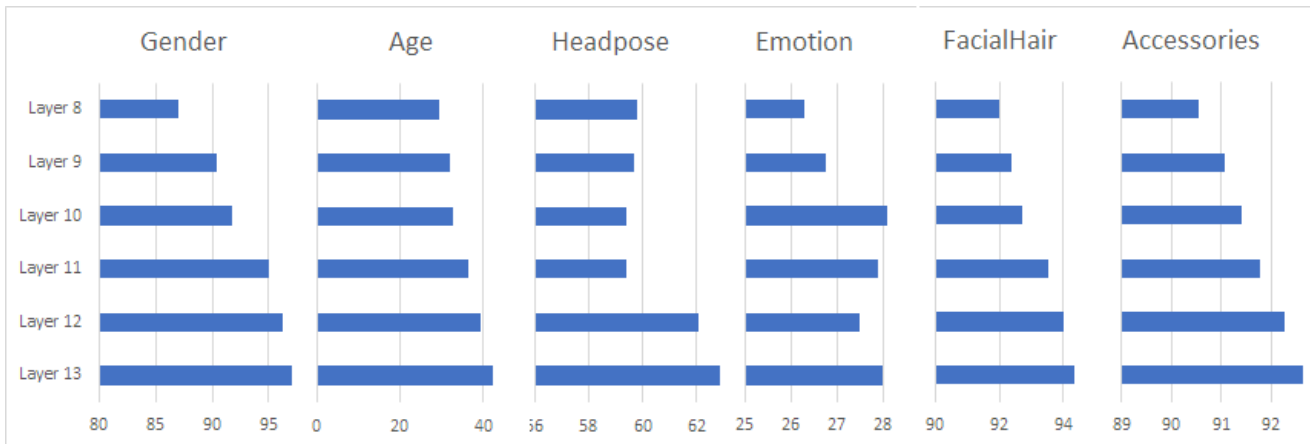


Figure 11. Figure shows the accuracy obtained by regressing the activations of the last 6 convolutional layers of face recognition network, VGG-Face, on various satellite tasks.

mately 760 GPU hours on Nvidia GeForce GTX 1080 Ti. In addition, we performed 1690 linear regression experiments on CPU. All codes were implemented in PyTorch Deep Learning Framework.

6. Conclusion

In this work, we explored several tasks in the face domain and their relationship to each other. Our proposed methodology, which uses a humble linear regression model, allowed us to leverage networks trained on large data sets, such as face recognition networks, for satellite tasks that

have less data, such as determining the age of a person, head pose, emotions, facial hair, accessories, etc. Our method provided a computationally simple method to adapt a pre-trained network for a task it was not trained for. We were able to estimate where the information was stored in the network and how well the features transferred from the primary task to the satellite task. These insights were used to prune networks for a specific task. Our results showed that it is possible to achieve high compression rates with a slight reduction of performance.

Type	Emotion		
	Filter size/stride,pad	Output size	#param
Conv2D	$3 \times 3 / 1,1$	$224 \times 224 \times 53$	5.9K
ReLU	-	$224 \times 224 \times 53$	-
Conv2D	$3 \times 3 / 1,1$	$224 \times 224 \times 44$	84.128K
ReLU	-	$224 \times 224 \times 44$	-
MaxPool	$2 \times 2 / 2,0$	$112 \times 112 \times 44$	-
Conv2D	$3 \times 3 / 1,1$	$112 \times 112 \times 80$	127.04K
ReLU	-	$112 \times 112 \times 80$	-
Conv2D	$3 \times 3 / 1,1$	$112 \times 112 \times 102$	294.16K
ReLU	-	$112 \times 112 \times 102$	-
MaxPool	$2 \times 2 / 2,0$	$56 \times 56 \times 102$	-
Conv2D	$3 \times 3 / 1,1$	$56 \times 56 \times 181$	665.35K
ReLU	-	$56 \times 56 \times 181$	-
Conv2D	$3 \times 3 / 1,1$	$56 \times 56 \times 170$	1108.4K
ReLU	-	$56 \times 56 \times 170$	-
Conv2D	$3 \times 3 / 1,1$	$56 \times 56 \times 203$	1243.17K
ReLU	-	$56 \times 56 \times 203$	-
MaxPool	$2 \times 2 / 2,0$	$28 \times 28 \times 203$	-
Conv2D	$3 \times 3 / 1,1$	$28 \times 28 \times 193$	1411.2K
ReLU	-	$28 \times 28 \times 193$	-
Conv2D	$3 \times 3 / 1,1$	$28 \times 28 \times 286$	1988.2K
ReLU	-	$28 \times 28 \times 286$	-
Conv2D	$3 \times 3 / 1,1$	$28 \times 28 \times 314$	3234.2K
ReLU	-	$28 \times 28 \times 314$	-
MaxPool	$2 \times 2 / 2,0$	$14 \times 14 \times 314$	-
Conv2D	$3 \times 3 / 1,1$	$14 \times 14 \times 218$	2465.1K
ReLU	-	$14 \times 14 \times 218$	-
Conv2D	$3 \times 3 / 1,1$	$14 \times 14 \times 237$	1860.9K
ReLU	-	$14 \times 14 \times 237$	-
Conv2D	$3 \times 3 / 1,1$	$14 \times 14 \times 225$	1920.6K
Avg. pool	-	225	-
Linear	-	7	6.3K

Table 6. The Architecture of VGG-Face network after pruning for emotion

References

[1] S. L. A. Dhall, R. Goecke and T. Gedeon. Collecting large, richly annotated facial-expression databases from movies. *IEEE MultiMedia*, 2012.

[2] G. Alain and Y. Bengio. Understanding intermediate layers using linear classifier probes. *CoRR*, 2016.

[3] Y. Aytar and A. Zisserman. Tabula rasa: Model transfer for object category detection. In *Computer Vision (ICCV), 2011 IEEE International Conference on*, 2011.

[4] D. Bau, B. Zhou, A. Khosla, A. Oliva, and A. Torralba. Network dissection: Quantifying interpretability of deep visual representations. In *Computer Vision and Pattern Recognition*, 2017.

[5] Y. Bengio. Deep learning of representations for unsupervised and transfer learning. In *Proceedings of ICML Workshop on Unsupervised and Transfer Learning*, 2012.

[6] Y. Bengio, A. Bergeron, N. Boulanger-Lewandowski, T. Breuel, Y. Chherawala, M. Cisse, D. Erhan, J. Eustache, X. Glorot, X. Muller, et al. Deep learners benefit more from out-of-distribution examples. In *Proceedings of the Fourteenth International Conference on Artificial Intelligence and Statistics*, 2011.

[7] R. Caruana. Learning many related tasks at the same time with backpropagation. In *Advances in neural information*

processing systems, 1995.

[8] A. Chattopadhyay, A. Sarkar, P. Howlader, and V. N. Balasubramanian. Grad-cam++: Generalized gradient-based visual explanations for deep convolutional networks. *2018 IEEE Winter Conference on Applications of Computer Vision (WACV)*, 2018.

[9] J. Donahue, Y. Jia, O. Vinyals, J. Hoffman, N. Zhang, E. Tzeng, and T. Darrell. Decaf: A deep convolutional activation feature for generic visual recognition. In *International conference on machine learning*, 2014.

[10] N. Gourier, D. Hall, and J. L. Crowley. Estimating face orientation from robust detection of salient facial features. In *ICPR International Workshop on Visual Observation of Deictic Gestures*, 2004.

[11] H. Han, A. K. Jain, S. Shan, and X. Chen. Heterogeneous face attribute estimation: A deep multi-task learning approach. *IEEE Transactions on Pattern Analysis and Machine Intelligence*, 2017.

[12] G. Hu, F. Yan, J. Kittler, W. Christmas, C. H. Chan, Z. Feng, and P. Huber. Efficient 3d morphable face model fitting. *Pattern Recognition.*, 2017.

[13] G. B. Huang, M. Ramesh, T. Berg, and E. Learned-miller. Labeled faces in the wild: A database for studying face recognition in unconstrained environments.

[14] P. Khorrani, T. L. Paine, and T. S. Huang. Do deep neural networks learn facial action units when doing expression recognition? In *Proceedings of the 2015 IEEE International Conference on Computer Vision Workshop (ICCVW)*, 2015.

[15] J. Kossaifi, G. Tzimiropoulos, S. Todorovic, and M. Pantic. A few-va database for valence and arousal estimation in-the-wild. *Image and Vision Computing*, 2017.

[16] H. Li, A. Kadav, I. Durdanovic, H. Samet, and H. Graf. Pruning filters for efficient convnets. In *Proceedings of the International Conference on Learning Representations (ICLR)*, 2017.

[17] J. J. Lim, R. R. Salakhutdinov, and A. Torralba. Transfer learning by borrowing examples for multiclass object detection. In *Advances in neural information processing systems*, 2011.

[18] Z. Liu, P. Luo, X. Wang, and X. Tang. Deep learning face attributes in the wild. In *Proceedings of International Conference on Computer Vision (ICCV)*, 2015.

[19] J. L. Long, N. Zhang, and T. Darrell. Do convnets learn correspondence? In *Advances in Neural Information Processing Systems*, 2014.

[20] A. T. Lopes, E. de Aguiar, A. F. D. Souza, and T. Oliveira-Santos. Facial expression recognition with convolutional neural networks: Coping with few data and the training sample order. *Pattern Recognition*, 2017.

[21] A. Mahendran and A. Vedaldi. Understanding deep image representations by inverting them. *Proceedings of the IEEE Conference on Computer Vision and Pattern Recognition*, 2015.

[22] P. M. R. Martin Koestinger, Paul Wohlhart and H. Bischof. Annotated Facial Landmarks in the Wild: A Large-scale, Real-world Database for Facial Landmark Localization. In *Proc. First IEEE International Workshop on Benchmarking Facial Image Analysis Technologies*, 2011.

- [23] A. Mordvintsev, C. Olah, and M. Tyka. Inceptionism: Going deeper into neural networks. *Google Research Blog*. Retrieved June, 2015.
- [24] S. Moschoglou, A. Papaioannou, C. Sagonas, J. Deng, I. Kotsia, and S. Zafeiriou. Agedb: the first manually collected, in-the-wild age database. In *Proceedings of IEEE Intl Conf on Computer Vision and Pattern Recognition (CVPR-W 2017)*, 2017.
- [25] A. Nguyen, J. Clune, Y. Bengio, A. Dosovitskiy, and J. Yosinski. Plug amp; play generative networks: Conditional iterative generation of images in latent space. In *2017 IEEE Conference on Computer Vision and Pattern Recognition (CVPR)*, 2017.
- [26] A. Nguyen, A. Dosovitskiy, J. Yosinski, T. Brox, and J. Clune. Synthesizing the preferred inputs for neurons in neural networks via deep generator networks. In *Advances in Neural Information Processing Systems*, 2016.
- [27] A. M. Nguyen, J. Yosinski, and J. Clune. Multifaceted feature visualization: Uncovering the different types of features learned by each neuron in deep neural networks. *CoRR*, 2016.
- [28] M. Oquab, L. Bottou, I. Laptev, and J. Sivic. Learning and transferring mid-level image representations using convolutional neural networks. In *Proceedings of the 2014 IEEE Conference on Computer Vision and Pattern Recognition*, 2014.
- [29] O. M. Parkhi, A. Vedaldi, and A. Zisserman. Deep face recognition. In *British Machine Vision Conference*, 2015.
- [30] M. Raghu, J. Gilmer, J. Yosinski, and J. Sohl-Dickstein. Svcca: Singular vector canonical correlation analysis for deep learning dynamics and interpretability. In *Advances in Neural Information Processing Systems*, 2017.
- [31] R. Ranjan, V. M. Patel, and R. Chellappa. Hyperface: A deep multi-task learning framework for face detection, landmark localization, pose estimation, and gender recognition. *IEEE Transactions on Pattern Analysis and Machine Intelligence*, 2017.
- [32] A. S. Razavian, H. Azizpour, J. Sullivan, and S. Carlsson. Cnn features off-the-shelf: An astounding baseline for recognition. In *Proceedings of the 2014 IEEE Conference on Computer Vision and Pattern Recognition Workshops*, 2014.
- [33] R. Rothe, R. Timofte, and L. V. Gool. Dex: Deep expectation of apparent age from a single image. In *IEEE International Conference on Computer Vision Workshops (ICCVW)*, 2015.
- [34] A. S. Morcos, D. G. T. Barrett, N. C. Rabinowitz, and M. Botvinick. On the importance of single directions for generalization. In *ICLR 2018*, 2018.
- [35] F. Schroff, D. Kalenichenko, and J. Philbin. Facenet: A unified embedding for face recognition and clustering. In *Proceedings of the IEEE conference on computer vision and pattern recognition*, 2015.
- [36] R. R. Selvaraju, M. Cogswell, A. Das, R. Vedantam, D. Parikh, and D. Batra. Grad-cam: Visual explanations from deep networks via gradient-based localization. In *2017 IEEE International Conference on Computer Vision (ICCV)*, 2017.
- [37] K. Simonyan, A. Vedaldi, and A. Zisserman. Deep inside convolutional networks: Visualising image classification models and saliency maps. *CoRR*, 2013.
- [38] K. Simonyan and A. Zisserman. Very deep convolutional networks for large-scale image recognition. *CoRR*, 2014.
- [39] J. T. Springenberg, A. Dosovitskiy, T. Brox, and M. Riedmiller. Striving for simplicity: The all convolutional net. *CoRR abs/1412.6806*, 2014.
- [40] C. Szegedy, W. Zaremba, I. Sutskever, J. Bruna, D. Erhan, I. J. Goodfellow, and R. Fergus. Intriguing properties of neural networks. *CoRR*, 2013.
- [41] R. Tibshirani. Regression shrinkage and selection via the lasso. *Journal of the Royal Statistical Society. Series B (Methodological)*, 1996.
- [42] T. Tommasi, F. Orabona, and B. Caputo. Safety in numbers: Learning categories from few examples with multi model knowledge transfer. In *Proceedings of IEEE Computer Vision and Pattern Recognition Conference*, 2010.
- [43] D. Wei, B. Zhou, A. Torrabi, and W. Freeman. Understanding intra-class knowledge inside cnn. *CoRR Vol abs/1507.02379*, 2015.
- [44] X. Wu, R. He, Z. Sun, and T. Tan. A light cnn for deep face representation with noisy labels. *IEEE Transactions on Information Forensics and Security*, 2018.
- [45] X. Yin and X. Liu. Multi-task convolutional neural network for pose-invariant face recognition. *IEEE Transactions on Image Processing*, 2018.
- [46] J. Yosinski, J. Clune, Y. Bengio, and H. Lipson. How transferable are features in deep neural networks? In *Proceedings of the 27th International Conference on Neural Information Processing Systems - Volume 2*, 2014.
- [47] A. R. Zamir, A. Sax, W. Shen, L. Guibas, J. Malik, and S. Savarese. Taskonomy: Disentangling task transfer learning. In *Proceedings of the IEEE Conference on Computer Vision and Pattern Recognition*, 2018.
- [48] Z. Zhang, P. Luo, C. C. Loy, and X. Tang. Facial landmark detection by deep multi-task learning. In D. Fleet, T. Pajdla, B. Schiele, and T. Tuytelaars, editors, *Computer Vision – ECCV 2014*, 2014.
- [49] B. Zhou, A. Khosla, À. Lapedriza, A. Oliva, and A. Torralba. Object detectors emerge in deep scene cnns. *CoRR*, 2014.
- [50] B. Zhou, A. Khosla, A. Lapedriza, A. Oliva, and A. Torralba. Learning deep features for discriminative localization. In *Computer Vision and Pattern Recognition (CVPR), 2016 IEEE Conference on*, 2016.
- [51] F. Zhu, H. Li, W. Ouyang, N. Yu, and X. Wang. Learning spatial regularization with image-level supervisions for multi-label image classification. In *Proceedings of the IEEE Conference on Computer Vision and Pattern Recognition*, 2017.